Advances in Colloid and Interface Science 225 (2015) 229–240

Contents lists available at ScienceDirect

Advances in Colloid and Interface Science

journal homepage: www.elsevier.com/locate/cis

Historical perspective

Magnetic graphene–carbon nanotube iron nanocomposites as adsorbents and antibacterial agents for water purification

Virender K. Sharma [a], Thomas J. McDonald [a], Hyunook Kim [b], Vijayendra K. Garg [c]

[a] Department of Environmental and Occupational Health, School of Public Health, Texas A&M University, College Station, TX 77843, USA
[b] Department of Environmental Engineering, The University of Seoul, 90 Jeonnong-dong Dongdaemun-gu, Seoul 130-743, Republic of Korea
[c] Institute of Physics, University of Brasília, 70919-970 Brasília, DF, Brazil

ARTICLE INFO

Available online 22 October 2015

Keywords:
Magnetic adsorbent
Carbon
Metals
Organics
Arsenic

ABSTRACT

One of the biggest challenges of the 21st century is to provide clean and affordable water through protecting source and purifying polluted waters. This review presents advances made in the synthesis of carbon- and iron-based nanomaterials, graphene–carbon nanotubes–iron oxides, which can remove pollutants and inactivate virus and bacteria efficiently in water. The three-dimensional graphene and graphene oxide based nanostructures exhibit large surface area and sorption sites that provide higher adsorption capacity to remove pollutants than two-dimensional graphene-based adsorbents and other conventional adsorbents. Examples are presented to demonstrate removal of metals (e.g., Cu, Pb, Cr(VI), and As) and organics (e.g., dyes and oil) by grapheme-based nanostructures. Inactivation of Gram-positive and Gram-negative bacterial species (e.g., *Escherichia coli* and *Staphylococcus aureus*) is also shown. A mechanism involving the interaction of adsorbents and pollutants is briefly discussed. Magnetic graphene-based nanomaterials can easily be separated from the treated water using an external magnet; however, there are challenges in implementing the graphene-based nanotechnology in treating real water.

Contents

1. Introduction

Reliable access to purified water devoid of toxins and microorganisms is one of the major global health issues of the 21st century. The current water supply systems in developing counties and industrialized nations face enormous pressure to provide access to clean drinking water sources [1–3]. Human activities contaminate natural source waters and consequently create water scarcity [4]. Rapid increase in global population, increasingly stringent water quality standards, and negative climate change effects on distribution of fresh water and supply as well as emerging contaminants in water put additional burden on water suppliers, and consequently lead to use of unconventional water sources such as brackish water and storm water [5]. More significantly, currently applied water and wastewater treatment technologies are not able to sustain the water quality and demand to meet requirements of

E-mail address: vsharma@tamhsc.edu (V.K. Sharma).

http://dx.doi.org/10.1016/j.cis.2015.10.006
0001-8686/

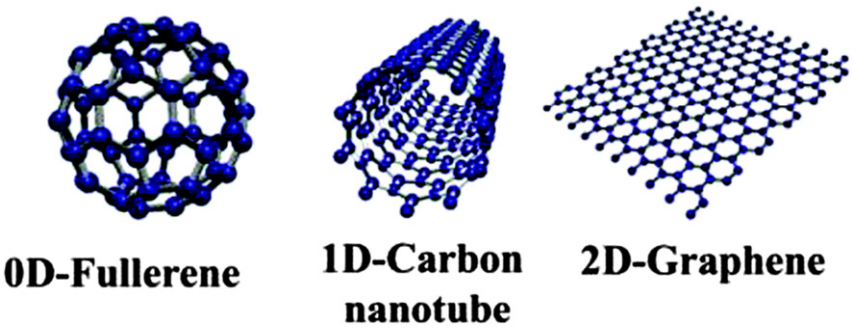

Fig. 1. Schematic illustration of the 0D (fullerene), 1D (carbon nanotube) and 2D (graphene) nanostructure of carbon based materials. Adapted from [170] with the permission of Royal Society of Chemistry.

environment and human health [6,7]. This paper presents adsorptive nanotechnology solution to fulfill next-generation demand of clean water supply.

Adsorption is usually applied to remove contaminants (inorganic and organic) in treatment of water and wastewater [8–11]. However, removal efficiency of adsorbents is limited by their surface area, active sites, non-selectivity, and slow adsorption kinetics. For example, activated carbon, which is applied commonly as adsorbent to treat polluted water is not able to remove pollutants to parts per billion (ppb) level [12]. The smart adsorbents are thus needed which can have excellent adsorption capacity to remove pollutants to the ppb level. Nanomaterials, which are normally defined as materials smaller than 100 nm, possess high specific surface area and strong sorption [13]. Nano-adsorbents can thus address shortcomings of conventional adsorbents [8,14–16]. Carbon-based nano-adsorbents with their high specific surface area and associated sorption sites and fast kinetics can enable technological innovation in advancing treatment efficiency of polluted water to provide clean and affordable water [5,17–20].

This review first presents current status of magnetic carbon-based nanomaterials and a progress made in their synthesis, followed by recent examples of applications of such nanostructures in removing metals and organics and in inactivating bacteria in water and wastewater.

2. Carbon-based nanomaterials

Carbon nanomaterials comprise of different allotropic forms of carbon that include fullerene, carbon nanotube (CNT), and graphene, which are zero-, one- and two-dimensional structures (Fig. 1). Graphene has two-dimensional (2D) structure material with atomic thickness having sp^2-bonded carbon atoms with honeycomb rings [21–25]. Graphene has a high surface-to-volume ratio because of its unique morphology and is ideal for many applications such as high performance electromagnetic interference, superior thermal conductivity, robustness, and a large theoretical specific surface area [26–33]. Graphene is thus a good candidate to be an effective adsorbent for removing contaminants in water [21, 22,34–45]. However, it encounters difficulties in recycling because it is not easily separable from the treated water. This problem can be circumvented by combining graphene with iron materials to make nanohybrid and to subsequently carry out magnetic separation. Iron oxides of varying valence states can promote the magnetic separation after the adsorption of pollutants from water [46–51].

Iron oxide nanoparticles are frequently used in removing metals in water [52–58]. However, removal efficiency of these nanoparticles is not high because of agglomeration. Other difficulty is the recycling of the nanoparticles having small sizes, particularly in a continuous flowing system. Embedded iron oxide nanoparticles on carbon-based nanomaterials which cost less and have high surface area is an attractive alternative. Examples include growth of iron oxide nanomaterials on graphene sheets [59]. The deposition of iron oxides onto graphene results in reduction on sorption sites on carbon surfaces; hence additional surfaces are required to increase sorption of pollutants on adsorbents. Unfortunately, the synthesized three-dimensional (3D) nanomaterial using this approach has low value because tubular metallic shapes on graphene reduce the specific surface area [60]. One approach of having smart carbon nanomaterial (SCNM) is the growth of 1D CNT on graphene and then subsequently decorated with iron oxide(s) to obtain 3-D nanostructures, which provide larger surface area. Fig. 2 shows such SCNM, which can have iron nanoparticles on surfaces of both graphene and CNTs [61]. Importantly, smart magnetic graphene (SMG) can be magnetic-separated easily after the water treatment.

2.1. Synthesis

The initial step to obtain SMG first involves the synthesis of graphene independently [26,62,63]. Graphene is also termed as reduced graphene oxide (RGO); its synthesis is usually from the reduction of graphene oxide (GO). Most of the workers applied Hummers' method to synthesize GO (HGO) from graphite [64]. In recent years, an improved method to synthesize GO (IGO) has also been proposed [65]. Fig. 3 summarizes both methods in which graphite were oxidized by a mixture of $KMnO_4$, H_2SO_4, and either $NaNO_3$ or H_3PO_4. In the modified HGO (HGO^+), larger amount of oxidant is applied; 6 M $KMnO_4$ is used in HGO^+ while 3 M $KMnO_4$ in HGO. The use of $NaNO_3$ in the Hummers' method generated toxic NO_2, therefore the IGO method using H_3PO_4 is relatively safer. Other important finding of IGO was the increased efficiency; indicated by the production of the very small amount of under-oxidized material after the synthesis. For example, 0.7 g of under-oxidized material was obtained from 3.0 g graphite in IGO

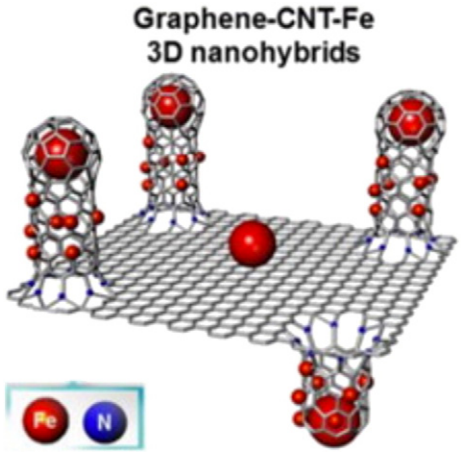

Fig. 2. Growth of carbon nanotubes and iron oxide nanoparticles on graphene surfaces. Adapted from [61] with the permission of the American Chemical Society.

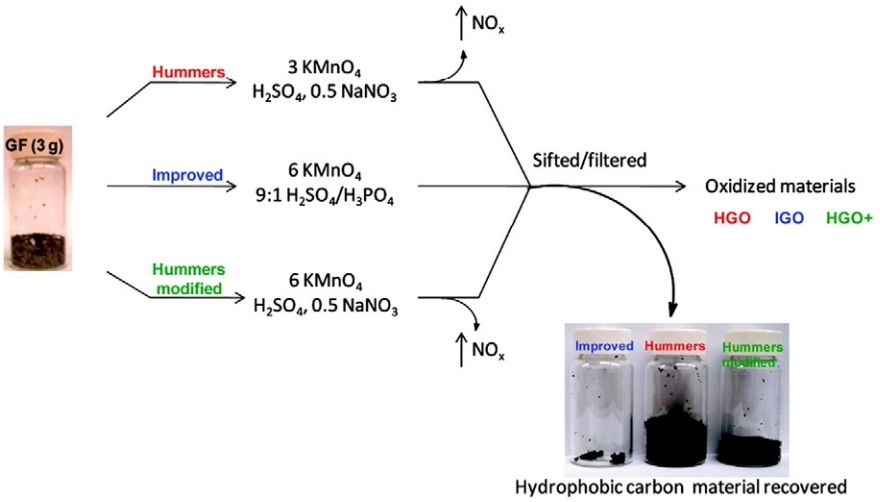

Fig. 3. Representation of the procedures followed starting with graphite flakes (GF). Under-oxidized hydrophobic carbon material recovered during the purification of IGO, HGO, and HGO+. The increased efficiency of the IGO method is indicated by the very small amount of under-oxidized material produced.
Adapted from [65] with the permission of the American Chemical Society.

while 6.7 g and 3.9 g were weight amounts of under-oxidized material in applications of HGO and HGO^+ methods. More details are in the original article [65].

More recently, potassium ferrate (K_2FeO_4) and H_2SO_4 were used as a mixing reagent to synthesize GO; designated as GO^{Fe} (Fig. 4) [66]. The FeO_4^{2-} is a strong oxidant and is a greener earth-abundant based compound [46,67–70]. The synthetic process of GO^{Fe} is completed in 1 h and has two main steps: intercalation–oxidation and oxidation–exfoliation. Significantly, this process can recover H_2SO_4 and is highly efficient.

Magnetic graphene-containing nanomaterials were synthesized using either graphene or GO as a precursor. Several researchers have used different approaches to build magnetic graphene and graphene–CNT nanostructures [17,18,62,71,72]. For example, ferrous and ferric ions were first precipitated on GO sheets, followed by reduction with sodium borohydrite ($NaBH_4$). Ascorbic acid and urea in combination with microwave radiation were also applied in order to establish green method to synthesize SMG. In another study, microwave radiation of GO and ferrocene ($Fe(_5H_5)_2$) precursors yielded SMG (Fig. 5) [62]. In this process, microwave irradiation led to reduction of GO and decomposition of ferrocene to give magnetic graphene. Ultrasonication and heating of precursors formed magnetic graphene, which is decorated with core@doble-shell nanoparticle [71].

Synthesis of 3D-graphene–CNT nanostructures has been performed only for the last few years [61,73,74]. Strategies of synthesizing the nanocomposites include the pyrolysis using urea as carbon source and microwave radiation [73]. The synergistic effects of ferrous ion in reduction of GO and acid-treated CNT yield the nanostructures in one-step reaction [74]. Dissolution of GO, azodicarbonamide (i.e., carbon source) and ferrocine (i.e., iron source) in acetonitrile and subsequent microwave irradiation results in 3D nanostructors. In the nanostructures, CNT grew on expanded graphene while iron oxide nanoparticles were on the surfaces of both graphene and CNT [61].

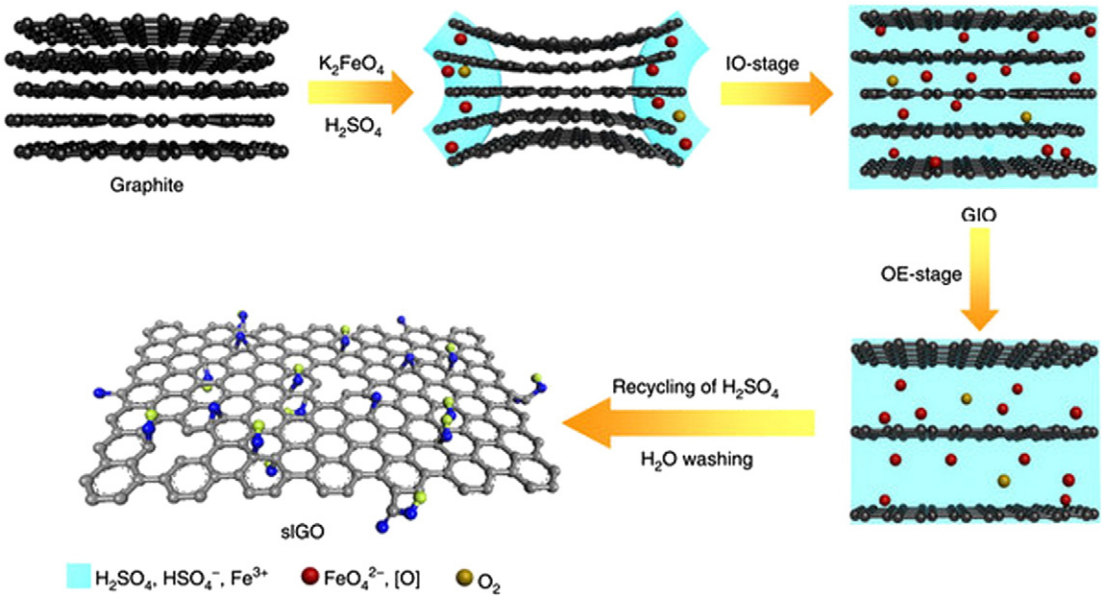

Fig. 4. Mechanism of GO^{Fe} synthesis with the oxidant of K_2FeO_4.
Adapted from [66] with permission of Nature Publishing Group.

2.2. Characterization

A number of analytical techniques have been applied to characterize synthesized SMG, which include elemental, thermal, surface and spectroscopy methods (Table 1) [29,52,75–80]. Different analysis is carried out to establish the element in the nanomaterials and use of preferable technique varies with the concentration and the target element [81]. Thermal analysis is useful in knowing the information on graphene-based catalysts [82]. The information obtained for dried powders is surface area and porosity measurements, which are usually the Brunauer–Emmett–Teller (BET) surface area and Barrett–Joyner–Halenda (BJH), respectively. Additionally, thermodesorption experiments can shed light on the small molecules evolved from the solid upon heating; characterized by adequate detectors (e.g., mass spectrometer) [80,83].

Transformation of graphite into graphite oxide can be studied by XRD patterns, which showed the change in the diffraction peak from 26.6° to 11.2° [76]. Nature of active site in graphene nanomaterials can be learned from the X-ray photoelectron spectroscopy (XPS) method [84]. Information on the elements can also be gained from the XPS technique. Morphology of the graphene based materials is established by imaging techniques, transmission electron microscopy (TEM), scanning electron microscopy (SEM), and atomic force microscopy (AFM). High resolution TEM (HRTEM) images demonstrates the hexagonal arrangement of the atoms in graphene [75–77,85]. Energy disperse X-ray spectroscopy (EDX) mapping can also be used to evaluate nanometric structures. Selected area electron diffraction (SAED) gives information about the crystallinity of graphene and other materials onto graphene such as Fe core and Fe_2O_3 shall in SMG materials [71]. An example of examination of 3D graphene–CNT–iron oxide (G–CNT–Fe) nanostructures using SEM images is shown in Fig. 6 [61]. Details of synthesis are provided elsewhere [61]. The expanded graphene worm is shown in Fig. 6(a). An image of iron oxide decorated graphene is presented in Fig. 6(b). In Fig. 6(c), the 3D structure of G–CNT–Fe is given. The CNT with a very high density is vertically grown (Fig. 6(c)). Significantly, the iron oxide nanoparticles are on the surfaces of both CNT and graphene. The aggregation of iron oxide nanoparticles on these surfaces is seen in ultrahigh resolution SEM Fig. 6(d).

IR spectroscopy has been commonly used to characterize graphene oxide while it cannot be applied for reduced GO and other graphene nanomaterials which do not exhibit strong any intense absorption vibrations in the IR. Comparatively, Raman spectroscopy is a very powerful technique to monitor the 2D, G ("graphenic") and D ("defects") bands present on graphene materials [76,77,84,86–88]. The solid NMR can also be used to monitor graphene oxide and reduced graphene oxide. Information on the functional groups on the materials can also be obtained using NMR technique [89].

3. Metals removal

Heavy metals, such as Cu, Pb, Cr(VI), As, and Hg, which are highly toxic pollutants in water resources and are of widespread concern. Pollution from these metals poses serious risks to human health through contamination of drinking water. Cu is essential, but also toxic metal; if exposed to excessive Cu, neuro-degeneration diseases, arteriosclerosis, or diabetes mellitus can be resulted in. Cu toxicity has been suggested to cause Alzheimer's diseases [90]. Pb is a pervasive environmental contaminant, which has adverse health effect on children and adults [91]. Pb can be ingested from different sources including paint, food, and drinking water, for example, release of Pb from drinking water service lines, which are made from lead materials [92]. Cr(VI) is of environmental concern due to its high toxicity and mobility; it is transported rapidly through the soil and aquatic environments [93,94]. Cr(VI) is carcinogenic and mutagenic and is also toxic to the environment. The United States Environmental Protection Agency (USEPA) is in the process of determining new federal maximum contaminant levels for Cr(VI) while California has established a public health goal of 0.02 μg L^{-1}. As contamination of groundwater represents a growing danger in many countries and imposes a huge detrimental impact on population's health. The As concentration in natural waters may vary from ~50 μg L^{-1} to >3000 μg L^{-1}; which is alarming if considering the As limit of 10 μg L^{-1} in drinking water, being suggested as the limiting safe-value by the World Health Organization [95]. In the aquatic environment, As is present as arsenite ($As^{III}O_3^{3-}$) and arsenate ($As^{V}O_4^{3-}$). As(III), which typically prevails in strongly reducing environments, is more mobile and therefore more toxic than As(V) [47,96–98]. Mercury is widely used in metallurgy, electronic industries, and mining industry and it is highly toxic [99]. In the environment, it can be accumulated in food chain and therefore will result in human health effects [100–102].

Graphene based nanomaterials have shown excellent adsorption ability to remove heavy metals in water [18,62,103–105]. Details regarding loading, the influence of pH, and concentration range of a number of toxic metals have been elegantly summarized [16,34,106]. For example, the adsorption capacity of graphene-based hydrogel was 373.8 mg g^{-1} for Pb(II), which is much higher than those of 15.6 mg g^{-1} and 40.0 mg g^{-1} for mesoporous γ-Fe_2O_3 and graphene sheets, respectively [107–109]. Graphene–CNT aerogels also have high adsorption capacity for removal of Pb(II) (i.e., 232–451 mg g^{-1}) [110]. Ren et al. [111] reported graphene material had much higher adsorption capacity for Cu(II) than that of the activated carbon. In their study, magnetic graphene oxide (MGO) composites could remove both Cu(II) and fulvic acids from aqueous solution via the inner-sphere surface complexation mechanism [112]. Nanohybrids of single-layer MGO had high adsorption properties for As(III) and As(V) [113,114]. Batch tests have shown that quartz sands coated with Fe_3O_4 and graphene oxide effectively remove As(III), As(V), Sb(III), and Hg(II) [115,116]. Magnetic graphene materials have shown high effectiveness to remove Cu(II), Pb(II), and Hg(II) [117–119].

A rapid removal of Fe(II) and Mn(II) from the polluted water using MGO has been demonstrated [104]. Interestingly, MGO with Fe and Mn adsorbed onto it (MGO–Fe and MGO–Mn) could be applied directly as new adsorbents for efficient removal of fluoride from water; fluoride is a common pollutant in numerous water sources [104]. Importantly, metal loaded MGO had higher adsorption capacity than the pure MGO (Fig. 7) [104]. This suggests that the adsorbed Fe and Mn played an important role in the adsorption of fluoride from the solution; confirming fluoride had stronger affinity to active adsorption sites in the metal-

Fig. 5. Microwave-assisted reduction and magnetization for the synthesis of magnetic graphene.
Adapted from [62] with the permission of the American chemical Society.

Table 1
Different techniques applied to characterized graphene-based materials.

Elemental analysis	Thermal analysis
Atomic absorption spectroscopy (AAS)	Thermogravimetry
Atomic emission spectroscopy (AES)	Thermodesorption
Inductively coupled plasma spectroscopy (ICP)	Differential scanning calorimetry
Combustion elemental analysis	
Energy dispersive X-ray	

Surface characterization	Spectroscopy
Brunauer–Emmett–Teller (BET)	Ultraviolet–visible (UV–Vis)
Barrett–Joyner–Halenda (BJH)	Fourier transform infrared (FTIR)
X-ray diffraction (XRD)	Raman
X-ray photoelectron spectroscopy (XPS)	Nuclear magnetic resonance (NMR)
Transmission electron microscopy (TEM)	
Scanning electron microscopy (SEM)	
Atomic force microscopy (AFM)	

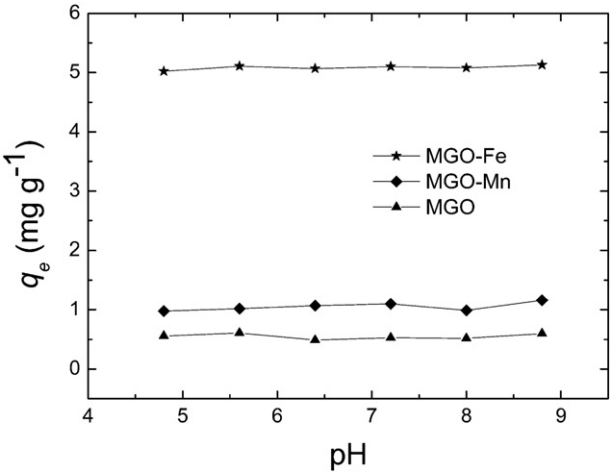

Fig. 7. pH dependence of the adsorption capacities of two metal-loaded MGOs and pure MGO for the removal of F at 298 K. The initial concentration of F was 19.0 mg L^{-1}. Adapted from [104] with the permission of the American Chemical Society.

loaded MGO than those of the pure MGO. Other finding was that higher amount of iron could be adsorbed onto MGO than that of the Mn; resulting in much higher fluoride up taken by MGO–Fe than by MGO–Mn (Fig. 6). No influence of pH in the range of 5.0–9.0 was seen on removal of fluoride for the studied adsorbents (Fig. 7).

Several studies have been carried out to remove Cr(VI) from aqueous solution using magnetic graphene composites, which had a much higher adsorption capacity than that of other adsorbents (Table 2) [62, 120–128]. Most of the measurements were made at near neutral pH and the parameter, q_m in Table 2 was derived from Langmuir and Freundlich models and more details are given in the original article [120]. The magnetic graphite oxide foam (GOF/Fe_2O_3) had a very large surface area of 564.2 m^2 g^{-1} to have high adsorption capacity (Table 2). A high magnetization of 40.2 emu g^{-1} was also obtained for GOF/Fe_3O_4. Significantly, magnetic graphene nanocomposites have shown fast complete removal of Cr(VI). For example, the removal of Cr(VI) from the wastewater could be achieved within 5 min using core@double-shell magnetic graphene nanoparticles [71]. The mechanism of adsorption of Cr(VI) on such nanoparticles was different from pure graphene. In the case of pure graphene, single-layer adsorption process occurs while an additional surface complexation process also

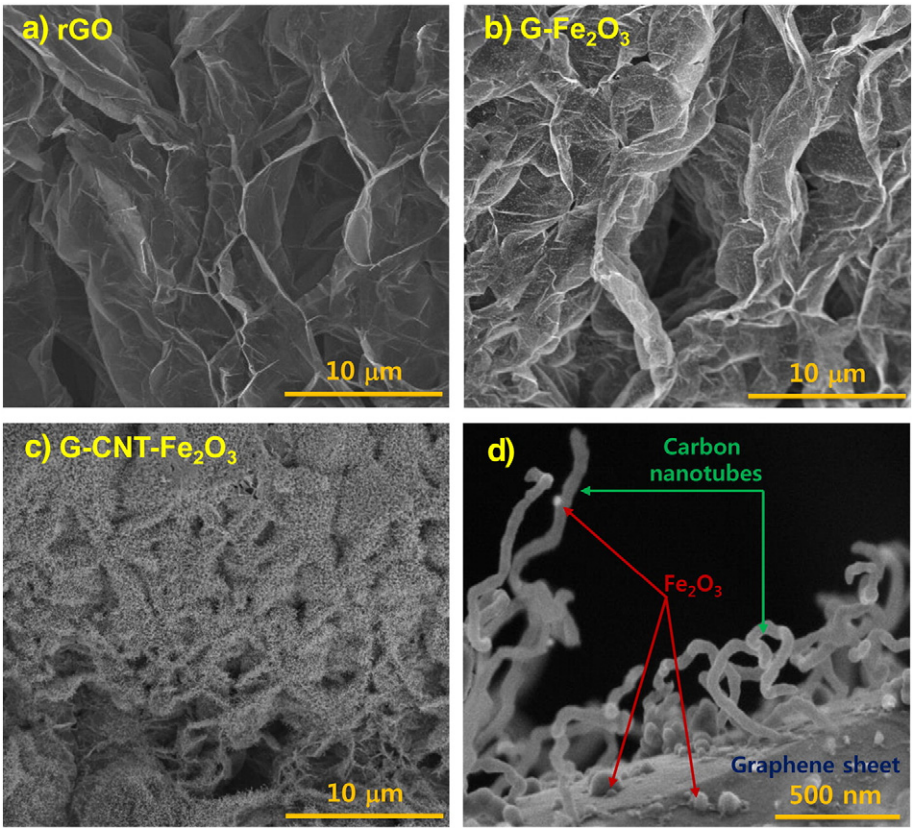

Fig. 6. SEM micrographs: (a) expanded graphene worm under microwave radiation, (b) 2D iron oxide decorated graphene, (c) graphene–carbon nanotube–iron oxide 3D nanostructures at the final stage, and (d) magnified 3D nanostructures; carbon nanotubes are vertically grown on graphene sheet and iron oxide nanoparticles and are decorated on both graphene sheet and carbon nanotubes.
Adapted from with the permission of the American Chemical Society [61].

Table 2
Comparison of the maximum adsorption capacities of some reported adsorbents for Cr(VI) removal.

Adsorbents	Surface area, $m^2\ g^{-1}$	Initial Cr(VI), $mg\ L^{-1}$	q_m, $mg\ g^{-1}$	Reference
Sugarcane bagasse	–	10–500	17.2	[121]
MnO-impregnated sand	9.21	20	18.8	[122]
CeO_2 hollow nanospheres	72	26.8	22.4	[123]
Flowerlike CeO_2	34.1	5.0–50	5.9	[124]
Polypyrrole/GO	–.a.	2.0	0.5	[125]
$Fe@Fe_2O_3$ nanowires	31.1	1.0–8.0	7	[126]
Graphene/Fe_3O_4	165	0.1–5.0	4.86–168	[62]
GOF/Fe_3O_4[a]	574	10–200	258.6	[120]
Graphene/polypyrrole	126.3	48.4	293.3	[127]
GO/MnO_2/Fe_3O_4	60.1	50–300	175.4	[128]

[a] GOF/Fe_3O_4—three dimensional graphene oxide foam/Fe_3O_4 nanocomposite.

happens during the adsorption on the magnetic graphene nanoparticles [71].

A recent work has demonstrated that the 3D graphene–CNT–iron oxide (3D G–CNT–Fe) nanostructures had higher adsorption capacity than the 2D iron-decorated graphene hybrids (2D G–Fe) [61,129]. As can be seen in Fig. 8 [61], the 3D G–CNT–Fe nanostructures had almost twice the adsorption capacity for As than 2D Ge–Fe hybrids at all concentrations of As. It seems that open pore structures and high meso-porosity of 3D G–CNT–Fe nanostructures promote its adsorption capacity for As. Furthermore, iron oxide nanoparticles in 3D G–CNT–Fe spatially and uniformly are dispersed on the surfaces of both graphene sheets and CNT, and provide active adsorption sites for As. Additionally, X-ray photoelectron spectroscopic measurements suggested a thickness of >3 nm for the arsenic-laden layer on the G–CNT–Fe surfaces, which was much higher than the monolayer thickness of arsenic–iron oxide surfaces. Overall, 3D magnetic graphene nanosurfaces are superior adsorbents to the conventional adsorbents in terms of removal efficiency for heavy metals.

4. Organics removal

Only limited studies have been reported to seek the removal of organics by magnetic graphene/graphene oxides and these were only for the past few years [8,16,16,72,130–146]. Most of the studies were carried out on removing dyes from water by magnetic graphene surfaces (Table 3) [8,16,72,136–146]. The studied dyes include ionic and organic dyes; they could be efficiently removed using magnetic

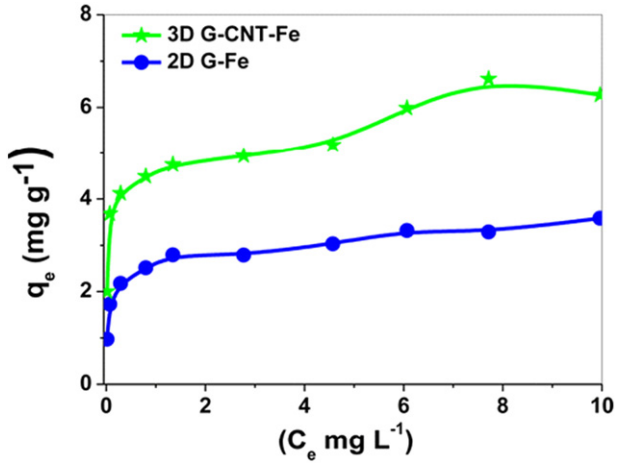

Fig. 8. Adsorption isotherms of 3D G–CNT–Fe nanostructures and 2D iron-decorated graphene for arsenic removal.
Adapted from [61] with the permission of the American Chemical Society.

graphene/graphene oxides. Other studied compounds include emerging contaminants such as antibiotics, tetrabromobisphenol, and endocrine disruptors (Table 3). The grafted chitosan copolymer was coated on magnetic graphene oxide (MGO), which was efficient to adsorb catechin [147]. Nanocomposites of polythiophene–graphene/Fe_3O_4 (G/Fe_3O_4@PT) have also been used in solid phase extraction of solvent, for example, extraction of polycyclic aromatic hydrocarbons from environmental water samples. In fact, G/Fe_3O_4@PT has a few advantages over G/Fe_3O_4 [148]. The van der Waals' forces and π–π stacking interactions have been suggested for the adsorption of organic molecules on magnetic graphene/graphene oxide [16].

A detailed mechanistic investigation of magnetic graphene composites was reported using naphthalene and its derivatives (naphthol and naphthylamine) [149]. The order of adsorption capacity over the acidic to basic pH range was determined as naphthalene < 1-naphthol < naphthylamine (Fig. 9) [149]. Significantly, the adsorption capacities of graphene oxide/$FeO \cdot Fe_2O_3$ for these compounds were approximately twice higher than those of $FeO \cdot Fe_2O_3$ nanoparticles [149]. Also, the adsorption was more than that of multi-walled CNTs/iron oxide, suggesting a role of adsorption morphology in adsorbing these aromatic compounds. Electron–donor–acceptor interactions were evoked to describe the trend of adsorption of compounds as shown in the Fig. 9.

In a recent study, 3D G-CNT aerogels were prepared, which had surface area of 315 $m^2\ g^{-1}$; it is much higher than that of graphene/Fe_3O_4 aerogels (110 $m^2\ g^{-1}$) [74,150,151]. The aerogels had excellent porosity and oleophillic properties due to incorporation of CNTs into the network. The adsorption capacity of aerogels was tested against gasoline (Fig. 10) [74]. Fig. 10a shows the adsorption rate of the aerogel. The adsorption rate of gasoline was very fast and the maximum adsorption capacity of ~34 $g\ g^{-1}$ was obtained within 5 min. Importantly, recycling of the aerogel was also carried out using suctioning of organics through vacuum system, followed by evaporation of organics through heating. Adsorbent was always removed after 60 min waiting period prior to recycling performance. The results showed that the aerogel had about 80% of its original adsorption capacity after eight cycles of recycle-testing (Fig. 10b). More importantly, SEM images of used aerogels had no structural damage. Another test showed the adsorption capacity of 28 g oil per g aerogel under continuous vacuum regime conditions [74]. This finding is significant because it indicates potential of the aerogel as filters for oil removal and hence in cleaning oil spill.

5. Antibacterial activity

Magnetic graphene-based nanocomposites as an antibacterial agent have been explored only recently [152–165]. Both graphene and CNT were combined independently with silver nanoparticles to obtain nanomaterials, which exhibited enhanced antibacterial activity against two strains of infectious bacteria such as *Escherichia coli* (*E. coli*, Gram-negative) and *Staphylococcus aureus* (*S. aureus*, Gram-positive) [162]. These combined materials were effective in controlling biofouling

Table 3
Removal of organic pollutants by magnetic graphite composites.

Pollutant	Adsorbent	Surface area $m^2\ g^{-1}$	Initial conc. $mg\ L^{-1}$	pH	q_m, $mg\ g^{-1}$	Reference
Dye	G/F_3O_4	94	50	1 M HCl	73.3	[136]
Dye	$G/F_3O_4G/F_3O_4$	256	20–60	6.6	198	[137]
Dye	Sulfonic G/Fe_3O_4	–	20–250	6.0	199–201	[138]
Dye	GO/Fe_3O_4/polyaniline	60	50–150	4.0	109–602	[139]
Dye	Cyclodextrin/GO/Fe	–	2–10	2.0–10.0	–	[140]
Dye	Citric acid/GO/Fe_3O_4	–	20	6.0	112	[141]
Dye	G/Fe_3O_4	–	5–40	–	65	[142]
Dye	GO/Fe	–	10	7.0	15–580	[8,143]
Tetrabromobishenol	G/iron oxide	–	–	7.0	38	[72]
Polychlorinated biphenyl	GO/Fe_3O_4	146	–	3–8	–	[144]
Endocrine disruptors	G/Fe_2O_3	210–300	5–100	7.0	200	[145]
Oil	G/Fe_3O_4	–	–	–	27.7	[169]
17β-Estradiol	GO/Fe_3O_4	171–204	5–10	7.0	87	[146]

control [166–168]. The large surface area of carbon-based materials and high catalytic activity of silver nanoparticles may have disinfected the infectious pathogens. Similar results were also observed in inactivation of *E. coli* using recycled graphene oxide–iron oxide–silver nanocomposites [156]. In another study, manganese graphene ferrite composites ($MnFe_2O_4$–G) showed higher antibacterial activity than graphene alone [154]. There was 82% reduction of *E. coli* in using $MnFe_2O_4$–G compared to 37% reduction when only graphene was used [154]. A separate study on the inactivation mechanism using MGO nanocomposites suggested deposition of nanomaterials on or penetration into cells of *E. coli*, causing destruction of cell integrity [155]. An examination of the cell during inactivation by SMG was conducted by Gollavelli et al. [62]. The result of their study is shown in Fig. 10 [62]. Increasing concentration of SMG could result in inactivation efficiency of 80% in minutes (Fig. 11A). The contact time of 1 h could result in disinfection efficiencies of ~90 and ~95% at SMG doses of 10 μg mL^{-1} and 20 μg mL^{-1}, respectively (Fig. 10a). The *E. coli* was stained with propidium iodide (PI) and 4′,6-diamidino-2-phenylindole (DAPI), and confocal images were collected (Fig. 11B). The image of the control cell is shown in Fig. 11ba in which blue color represents bacterial cells permeable only to DAPI but not to PI (red color). Fig. 11ba suggests that most of the cells were alive in control. However, addition of 10 μg mL^{-1} could disinfect most of the cells (Fig. 11ba).

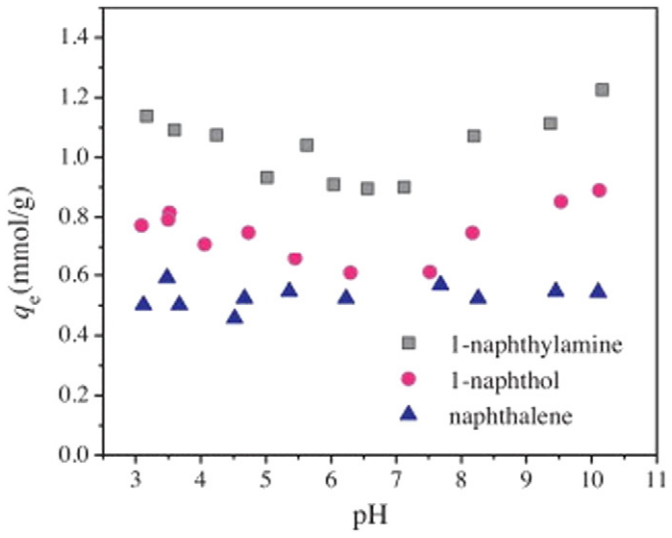

Fig. 9. Effect of pH on the adsorption of 1-naphthylamine, 1-naphthol and naphthalene on $GO/FeO{\cdot}Fe_2O_3$. m/V = 0.1 g L^{-1}, pH = 7.0 ± 0.1, I = 0.01 M $NaClO_4$. T = 283.15 K. The initial concentration for 1-naphthalene and 1-naphthol is 0.139 mmol/L and initial concentration for naphthalene is 0.156 mmol L^{-1}, respectively.
Adapted from [149] with the permission of Elsevier.

Removal of a wide range of Gram-positive and Gram-negative bacterial species and bacteriophage MS2 was tested with magnetic Fe_3O_4/graphene composite (G–Fe_3O_4) (Fig. 12) [157]. Removal experiments were carried out by applying three nanosurfaces, i.e., G–Fe_3O_4, GO, and Fe_3O_4 at pH 7.0 and the initial adsorbent concentration in solution was 0.25 mg mL^{-1}. The removal efficiencies for Gram-positive were 88.5, 92.8, and 92.3% for *S. aureus*, *E. faecalis*, and *E. faecalis*, respectively whereas 93.1, 60.5, and 82.5% were removal efficiencies for three Gram-negative species, i.e., *E. coli*, *Shigella*, and *Salmonella*, respectively. Graphene also had high removal efficiencies of the bacterial species, but G–Fe_3O_4 nanocomposites can provide added advantage over graphene only using their magnetic force for separation. Comparatively, the removal efficiency of pure Fe_3O_4 was lower than G–Fe_3O_4 composites. The removal efficiency of *bacteriophage MS2* by G–Fe_3O_4 was also high (97.8%) (Fig. 12). Removal efficiency of G–Fe_3O_4 for microorganisms in river water samples was 94.8 and 96.3% for bacteria and bacteriophage species, respectively [157].

6. Conclusions and future outlook

The development of facile graphene nanomaterials has made a significant progress over the past few years and the current focus is on synthesizing magnetic graphene nanomaterials which have a large surface area. Graphite sheets have been usually main precursors to synthesize first graphene oxide using Hummer/modified Hummer methods, which were then reduced to graphene. Iron oxides were then deposited on graphene/graphene oxide. CNT has also been grown using a microwave radiation in this step in which both graphene and graphene oxide were initial carbon materials and 3D nanostructures were obtained having a large surface area and sorption sites. Further increase in adsorption capacity of 3D nanostructures can be achieved by having functionality on the surface of the nanomaterials. Greener approaches to produce the nanostructures by applying easily and naturally available agents such as chitosan and vitamins and by using microwave irradiation may be included. Most of the magnetic graphenes have used iron oxide as Fe_2O_3. In the future, therefore, different sources of iron salts such as Fe_3O_4, FeOOH, and FeO_2^- may be explored. The uniformity of iron oxides can be finely tuned in order to enhance its magnetic property to maximize the magnetic recovery of the composite. Development of magnetic Fe_3O_4 nanoparticles with controlled morphology may be advantageous.

The purification of water from various pollutants is challenging and graphene-based nanostructures can deliver simple and effective decontamination/disinfection of water. Results are forthcoming which show that the magnetic graphene/graphene oxides are new generation of materials for pollution management. These materials have outstanding adsorption capacity to result in efficient removal of ionic and organic heavy metals. Magnetic graphene has also antibacterial effectiveness

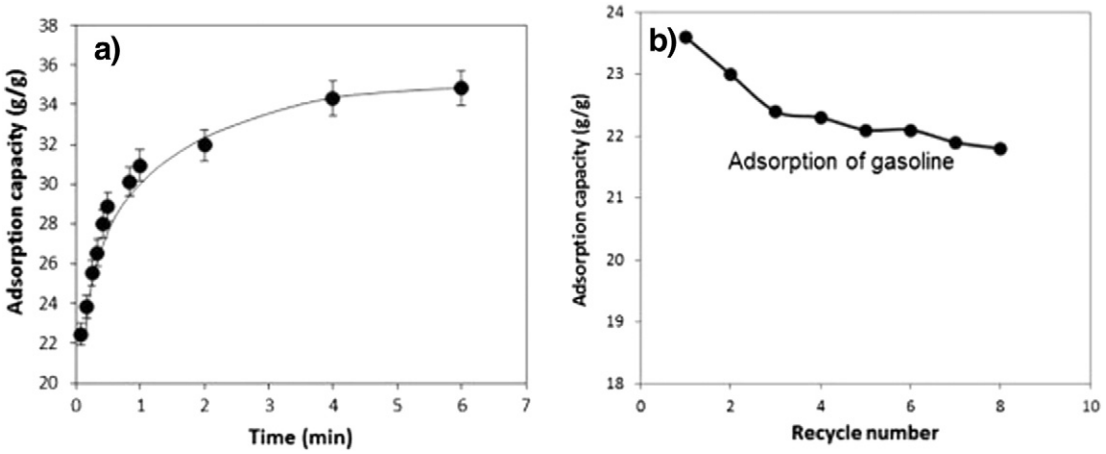

Fig. 10. (a) Rate of adsorption and (b) recycling performance of the gasoline adsorption capacity of graphene–CNT aerogel. Adapted from [74] with the permission of Elsevier.

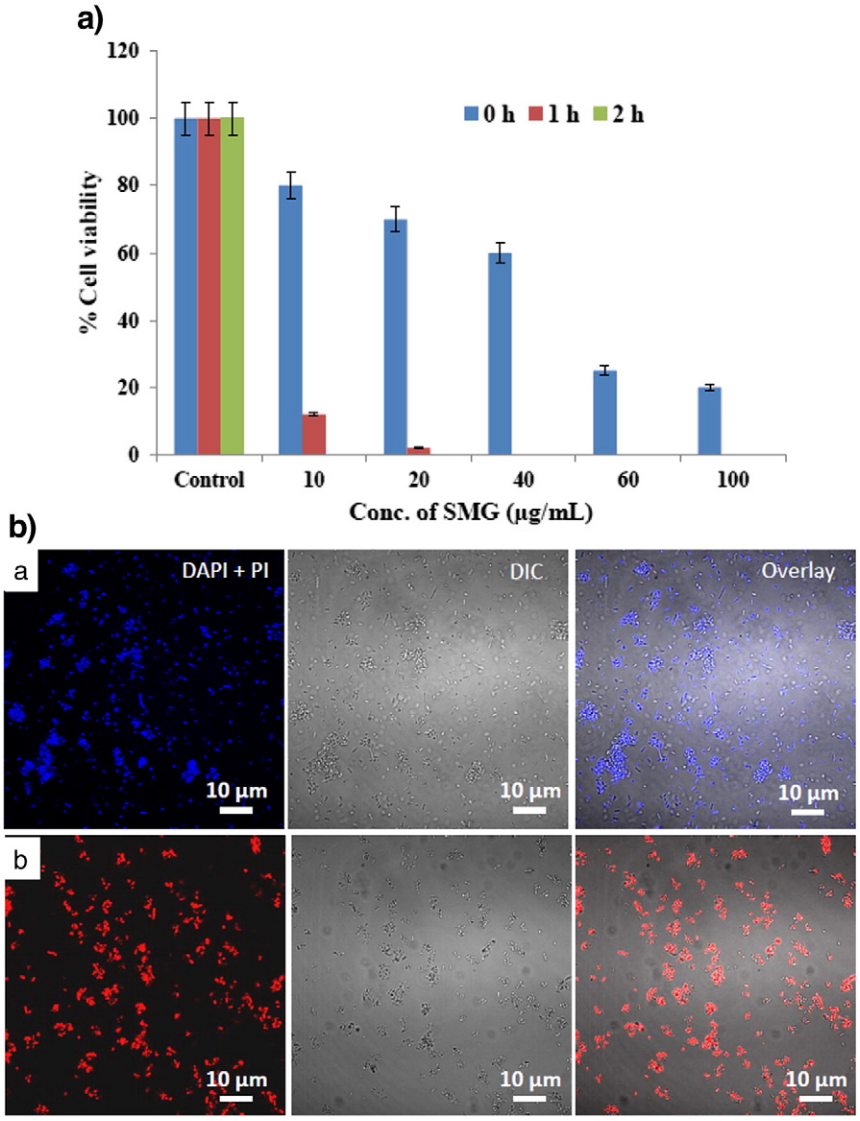

Fig. 11. Interaction time and SMG concentration dependent disinfection control by SMG toward *E. coli*. (A) Cell viability obtained by plate count method and (B) confocal microscopy images for (a) control and (b) experimental (10 μg mL^{-1} SMG) stained with DAPI (blue color) and PI (red color).
Reproduced from [62] with the permission of the American Chemical Society.

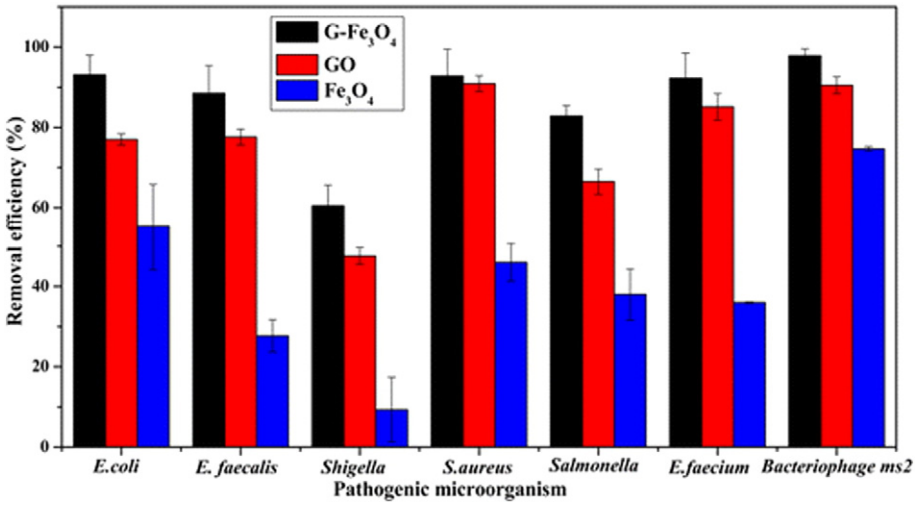

Fig. 12. Nonspecific removal of *bacteriophage MS2*, *E. coli*, *E. faecalis*, *Shigella*, *S. aureus*, *Salmonella*, *E. faecium*. Adapted from [157] with the American Chemical Society.

toward both Gram-positive and Gram-negative bacteria. In addition, graphene–CNT–iron oxide nanomaterials can be multifunctional agents in numerous areas ranging from environmental remediation to healthcare.

Almost all the studies to seek efficient removal of pollutants have been performed using deionized water, but potential of magnetic graphene and CNT nanomaterials needs to be demonstrated under real water conditions. In wastewater, carbonate, phosphate, and silicate can successfully compete with target metals/organics for sorption sites of nanostructures. Other important constituent of source waters and wastewater is natural organic matters, e.g., fulvic and humic acids which will occupy graphene and CNT surfaces and will, therefore, influence adsorption of pollutants on nanostructures. The validity of the graphene-based nanotechnology shall be evaluated under real water conditions.

Acknowledgments

H. Kim acknowledges the support of the R&D Program of MOTI/KEIT (R&D program number: 10037331, Development of Core Water Treatment Technologies based on Intelligent BT-NT-IT Fusion Platform).

References

[1] Qu X, Brame J, Li Q, Alvarez PJJ. Nanotechnology for a safe and sustainable water supply: enabling integrated water treatment and reuse. Acc Chem Res 2013;46:834–43.
[2] Shannon MA, Bohn PW, Elimelech M, Georgiadis JG, Marias BJ, Mayes AM. Science and technology for water purification in the coming decades. Nature 2008;452:301–10.
[3] Liu J, Yang W. Water sustainability for China and beyond. Science 2012;337:649–50.
[4] Brookes JD, Carey CC, Hamilton DP, Ho L, Van Der Linden L, Renner R, et al. Emerging challenges for the drinking water industry. Environ Sci Technol 2014;48:2099–101.
[5] Qu X, Alvarez PJJ, Li Q. Applications of nanotechnology in water and wastewater treatment. Water Res 2013;47:3931–46.
[6] Schwarzenbach RP, Escher BI, Fenner K, Hofstetter TB, Johnson CA, Von Gunten U, et al. The challenge of micropollutants in aquatic systems. Science 2006;313:1072–7.
[7] Sedlak DL, Von Gunten U. The chlorine dilemma. Science 2011;331:42–3.
[8] Kyzas GZ, Matis KA. Nanoadsorbents for pollutants removal: a review. J Mol Liq 2015;203:159–68.
[9] Zhang Y, He Z, Wang H, Qi L, Liu G, Zhang X. Applications of hollow nanomaterials in environmental remediation and monitoring: a review. Front Environ Sci Eng 2015;9:770–83.
[10] Carpenter AW, De Lannoy C, Wiesner MR. Cellulose nanomaterials in water treatment technologies. Environ Sci Technol 2015;49:5277–87.
[11] Gehrke I, Geiser A, Somborn-Schulz A. Innovations in nanotechnology for water treatment. Nanotechnol Sci Appl 2015;8.
[12] Pillay K, Cukrowska EM, Coville NJ. Multi-walled carbon nanotubes as adsorbents for the removal of parts per billion levels of hexavalent chromium from aqueous solution. J Hazard Mater 2009;166:1067–75.
[13] Sharma VK, Filip J, Zboril R, Varma RS. Natural inorganic nanoparticles; formation, fate, and toxicity in the environment. Chem Soc Rev 2015 [in press].
[14] Trujillo-Reyes J, Peralta-Videa JR, Gardea-Torresdey JL. Supported and unsupported nanomaterials for water and soil remediation: are they a useful solution for worldwide pollution? J Hazard Mater 2014;280:487–503.
[15] Kurniawan TA, Sillanpää MET, Sillanpää M. Nanoadsorbents for remediation of aquatic environment: local and practical solutions for global water pollution problems. Crit Rev Environ Sci Technol 2012;42:1233–95.
[16] Yu J, Yu L, Yang H, Liu Q, Chen X, Jiang X, et al. Graphene nanosheets as novel adsorbents in adsorption, preconcentration and removal of gases, organic compounds and metal ions. Sci Total Environ 2015;502:70–9.
[17] Fang Q, Shen Y, Chen B. Synthesis, decoration and properties of three-dimensional graphene-based macrostructures: a review. Chem Eng J 2015;264:753–71.
[18] Shen Y, Fang Q, Chen B. Environmental applications of three-dimensional graphene-based macrostructures: adsorption, transformation, and detection. Environ Sci Technol 2015;49:67–84.
[19] Kim H, Hwang YS, Sharma VK. Adsorption of antibiotics and iopromide onto single-walled and multi-walled carbon nanotubes. Chem Eng J 2014;255:23–7.
[20] Jurado-Sánchez B, Sattayasamitsathit S, Gao W, Santos L, Fedorak Y, Singh VV, et al. Self-propelled activated carbon janus micromotors for efficient water purification. Small 2015;11:499–506.
[21] Allen MJ, Tung VC, Kaner RB. Honeycomb carbon: a review of graphene. Chem Rev 2010;110:132–45.
[22] Xu M, Liang T, Shi M, Chen H. Graphene-like two-dimensional materials. Chem Rev 2013;113:3766–98.
[23] Kim J, Kwon S, Cho D, Kang B, Kwon H, Kim Y, et al. Direct exfoliation and dispersion of two-dimensional materials in pure water via temperature control. Nat Commun 2015;6 [Article number: 8294].
[24] Vo TH, Perera UGE, Shekhirev M, Mehdi Pour M, Kunkel DA, Lu H, et al. Nitrogen-doping induced self-assembly of graphene nanoribbon-based two-dimensional and three-dimensional metamaterials. Nano Lett 2015;15:5770–7.
[25] Matsumoto M, Saito Y, Park C, Fukushima T, Aida T. Ultrahigh-throughput exfoliation of graphite into pristine 'single-layer' graphene using microwaves and molecularly engineered ionic liquids. Nat Chem 2015;7:730–6.
[26] Wang X, Liu B, Lu Q, Qu Q. Graphene-based materials: fabrication and application for adsorption in analytical chemistry. J Chromatogr A 2014;1362:1–15.
[27] Urbanova V, Magro M, Gedanken A, Baratella D, Vianello F, Zboril R. Nanocrystalline iron oxides, composites, and related materials as a platform for electrochemical, magnetic, and chemical biosensors. Chem Mater 2014;26:6653–73.
[28] Wang H, Li S, Si Y, Sun Z, Li S, Lin Y. Recyclable enzyme mimic of cubic Fe_3O_4 nanoparticles loaded on graphene oxide-dispersed carbon nanotubes with enhanced peroxidase-like catalysis and electrocatalysis. J Mater Chem B 2014;2:4442–8.
[29] Gu W, Deng X, Gu X, Jia X, Lou B, Zhang X, et al. Stabilized, superparamagnetic functionalized graphene/Fe_3O_4@Au nanocomposites for a magnetically-controlled solid-state electrochemiluminescence biosensing application. Anal Chem 2015;87:1876–81.
[30] Tripathi P, Prakash Patel CR, Dixit A, Singh AP, Kumar P, Shaz MA, et al. High yield synthesis of electrolyte heating assisted electrochemically exfoliated graphene for electromagnetic interference shielding applications. RSC Adv 2015;5:19074–81.
[31] Singh AP, Mishra M, Hashim DP, Narayanan TN, Hahm MG, Kumar P, et al. Probing the engineered sandwich network of vertically aligned carbon nanotube-reduced

graphene oxide composites for high performance electromagnetic interference shielding applications. Carbon 2015;85:79–88.
[32] Prasad KP, Chen Y, Chen P. Three-dimensional graphene-carbon nanotube hybrid for high-performance enzymatic biofuel cells. ACS Appl Mater Interfaces 2014;6:3387–93.
[33] Chen Y, Prasad KP, Wang X, Pang H, Yan R, Than A, et al. Enzymeless multi-sugar fuel cells with high power output based on 3D graphene–Co_3O_4 hybrid electrodes. Phys Chem Chem Phys 2013;15:9170–6.
[34] Chowdhury S, Balasubramanian R. Recent advances in the use of graphene-family nanoadsorbents for removal of toxic pollutants from wastewater. Adv Colloid Interface Sci 2014;204:35–56.
[35] Cheng C, Deng J, Lei B, He A, Zhang X, Ma L, et al. Toward 3D graphene oxide gels based adsorbents for high-efficient water treatment via the promotion of biopolymers. J Hazard Mater 2013;263:467–78.
[36] Mahmoud KA, Mansoor B, Mansour A, Khraisheh M. Functional graphene nanosheets: the next generation membranes for water desalination. Desalination 2015;356:208–25.
[37] Pavagadhi S, Tang ALL, Sathishkumar M, Loh KP, Balasubramanian R. Removal of microcystin-LR and microcystin-RR by graphene oxide: adsorption and kinetic experiments. Water Res 2013;47:4621–9.
[38] Gao P, Liu Z, Sun DD, Ng WJ. The efficient separation of surfactant-stabilized oil–water emulsions with a flexible and superhydrophilic graphene–TiO_2 composite membrane. J Mater Chem A 2014;2:14082–8.
[39] Liu L, Bai H, Liu J, Sun DD. Multifunctional graphene oxide–TiO_2–Ag nanocomposites for high performance water disinfection and decontamination under solar irradiation. J Hazard Mater 2013;261:214–23.
[40] Ciriminna R, Zhang N, Yang M, Meneguzzo F, Xu Y, Pagliaro M. Commercialization of graphene-based technologies: a critical insight. Chem Commun 2015;51:7090–5.
[41] Zhang C, Zhang RZ, Ma YQ, Guan WB, Wu WB, Liu X, et al. Preparation of cellulose/graphene composite and its applications for triazine pesticides from water. ACS Sustain Chem Eng 2015;3:396–405.
[42] Tseng W, Hsu K, Shiea CS, Huang Y. Recent trends in nanomaterial-based microanalytical systems for the speciation of trace elements: a critical review. Anal Chim Acta 2015;884:1–18.
[43] Zhang F, Song Y, Song S, Zhang R, Hou W. Synthesis of magnetite–graphene oxide-layered double hydroxide composites and applications for the removal of Pb(II) and 2,4-dichlorophenoxyacetic acid from aqueous solutions. ACS Appl Mater Interfaces 2015;7:7251–63.
[44] Jiang T, Yan L, Zhang L, Li Y, Zhao Q, Yin H. Fabrication of a novel graphene oxide/ß-FeOOH composite and its adsorption behavior for copper ions from aqueous solution. Dalton Trans 2015;44:10448–56.
[45] Yan L, Zhao Q, Jiang T, Liu X, Li Y, Fang W, et al. Adsorption characteristics and behavior of a graphene oxide–Al13 composite for cadmium ion removal from aqueous solutions. RSC Adv 2015;5:67372–9.
[46] Sharma VK, Zboril R, Varma RS. Ferrates: greener oxidants with multimodal actions in water treatment technologies. Acc Chem Res 2015;48:182–91.
[47] Prucek R, Tucek J, Kolarík J, Hušková I, Filip J, Varma RS, et al. Ferrate(VI)-prompted removal of metals in aqueous media: mechanistic delineation of enhanced efficiency via metal entrenchment in magnetic oxides. Environ Sci Technol 2015;49:2319–27.
[48] Santhosh C, Kollu P, Doshi S, Sharma M, Bahadur D, Vanchinathan MT, et al. Adsorption, photodegradation and antibacterial study of graphene–Fe_3O_4 nanocomposite for multipurpose water purification application. RSC Adv 2014;4:28300–8.
[49] Paulus A, Fischer I, Hobley TJ, Franzreb M. Use of continuous magnetic extraction for removal of feedstock contaminants in flow-through mode. Sep Purif Technol 2014;127:174–80.
[50] Hu X, Liu Y, Wang H, Chen A, Zeng G, Liu S, et al. Removal of Cu(II) ions from aqueous solution using sulfonated magnetic graphene oxide composite. Sep Purif Technol 2013;108:189–95.
[51] McCoy TM, Brown P, Eastoe J, Tabor RF. Noncovalent magnetic control and reversible recovery of graphene oxide using iron oxide and magnetic surfactants. ACS Appl Mater Interfaces 2014;7:2124–33.
[52] Giakisikli G, Anthemidis AN. Magnetic materials as sorbents for metal/metalloid preconcentration and/or separation. A review. Anal Chim Acta 2013;789:1–16.
[53] Saharan P, Chaudhary GR, Mehta SK, Umar A. Removal of water contaminants by iron oxide nanomaterials. J Nanosci Nanotechnol 2014;14:627–43.
[54] Shahriari T, Nabi Bidhendi G, Mehrdadi N, Torabian A. Effective parameters for the adsorption of chromium(III) onto iron oxide magnetic nanoparticle. Int J Environ Sci Technol 2014;11:349–56.
[55] Machala L, Filip J, Prucek R, Tucek J, Frydrych J, Sharma VK, et al. Potassium ferrite ($KFeO_2$): synthesis, decomposition, and application for removal of metals. Sci Adv Mater 2015;7:579–87.
[56] Casbeer E, Sharma VK, Li X. Synthesis and photocatalytic activity of ferrites under visible light: a review. Sep Purif Technol 2012;87:1–14.
[57] Hazra S, Ghosh NN. Preparation of nanoferrites and their applications. J Nanosci Nanotechnol 2014;14:1983–2000.
[58] Chen B, Zhu Z, Ma J, Qiu Y, Chen J. Iron oxide supported sulfhydryl-functionalized multiwalled carbon nanotubes for removal of arsenite from aqueous solution. ChemPlusChem 2015;80:740–8.
[59] Haham H, Grinblat J, Sougrati M, Stievano L, Margel S. Engineering of iron-based magnetic activated carbon fabrics for environmental remediation. Materials 2015;8:4593–607.
[60] Zhang Z, Zou R, Song G, Yu L, Chen Z, Hu J. Highly aligned SnO_2 nanorods on graphene sheets for gas sensors. J Mater Chem 2011;21:17360–5.
[61] Vadahanambi S, Lee S, Kim W, Oh I. Arsenic removal from contaminated water using three-dimensional graphene–carbon nanotube–iron oxide nanostructures. Environ Sci Technol 2013;47:10510–7.
[62] Gollavelli G, Chang C, Ling Y. Facile synthesis of smart magnetic graphene for safe drinking water: heavy metal removal and disinfection control. ACS Sustain Chem Eng 2013;1:462–72.
[63] Sun J, Yang N, Sun Z, Zeng M, Fu L, Hu C, et al. Fully converting graphite into graphene oxide hydrogels by preoxidation with impure manganese dioxide. ACS Appl Mater Interfaces 2015;7:21356–63.
[64] Hummers Jr WS, Offeman RE. Preparation of graphitic oxide. J Am Chem Soc 1958;80:1339.
[65] Marcano DC, Kosynkin DV, Berlin JM, Sinitskii A, Sun Z, Slesarev A, et al. Improved synthesis of graphene oxide. ACS Nano 2010;4:4806–14.
[66] Peng L, Xu Z, Liu Z, Wei Y, Sun H, Li Z, et al. An iron-based green approach to 1-h production of single-layer graphene oxide. Nat Commun 2015;6:5716.
[67] Casbeer EM, Sharma VK, Zajickova Z, Dionysiou DD. Kinetics and mechanism of oxidation of tryptophan by ferrate(VI). Environ Sci Technol 2013;47:4572–80.
[68] Al-Abduly A, Sharma VK. Oxidation of benzothiophene, dibenzothiophene, and methyl-dibenzothiophene by ferrate(VI). J Hazard Mater 2014;279:296–301.
[69] Osathaphan K, Kittisarn W, Chatchaitanawat P, Yngard RA, Kim H, Sharma VK. Oxidation of Ni(II)-cyano and Co(III)-cyano complexes by ferrate(VI): effect of pH. J Environ Sci Health A Tox Hazard Subst Environ Eng 2014;49:1380–4.
[70] Yates BJ, Darlington R, Zboril R, Sharma VK. High-valent iron-based oxidants to treat perfluorooctanesulfonate and perfluorooctanoic acid in water. Environ Chem Lett 2014:413–7.
[71] Zhu J, Wei S, Gu H, Rapole SB, Wang Q, Luo Z, et al. One-pot synthesis of magnetic graphene nanocomposites decorated with core@double-shell nanoparticles for fast chromium removal. Environ Sci Technol 2012;46:977–85.
[72] Thakur S, Karak N. One-step approach to prepare magnetic iron oxide/reduced graphene oxide nanohybrid for efficient organic and inorganic pollutants removal. Mater Chem Phys 2014;144:425–32.
[73] Wang L, Huang Y, Li C, Chen J, Sun X. A facile one-pot method to synthesize a three-dimensional graphene@carbon nanotube composite as a high-efficiency microwave absorber. Phys Chem Chem Phys 2015;17:2228–34.
[74] Kabiri S, Tran DNH, Altalhi T, Losic D. Outstanding adsorption performance of graphene–carbon nanotube aerogels for continuous oil removal. Carbon 2014;80:523–33.
[75] Navalon S, Dhakshinamoorthy A, Alvaro M, Garcia H. Carbocatalysis by graphene-based materials. Chem Rev 2014;114:6179–212.
[76] Kuila T, Bose S, Mishra AK, Khanra P, Kim NH, Lee JH. Chemical functionalization of graphene and its applications. Prog Mater Sci 2012;57:1061–105.
[77] Soldano C, Mahmood A, Dujardin E. Production, properties and potential of graphene. Carbon 2010;48:2127–50.
[78] Singh V, Joung D, Zhai L, Das S, Khondaker SI, Seal S. Graphene based materials: past, present and future. Prog Mater Sci 2011;56:1178–271.
[79] Tunckol M, Durand J, Serp P. Carbon nanomaterial-ionic liquid hybrids. Carbon 2012;50:4303–34.
[80] Montes-Navajas P, Asenjo NG, Santamaría R, Menéndez R, Corma A, García H. Surface area measurement of graphene oxide in aqueous solutions. Langmuir 2013;29:13443–8.
[81] Lee T, Min SH, Gu M, Jung YK, Lee W, Lee JU, et al. Layer-by-layer assembly for graphene-based multilayer nanocomposites: synthesis and applications. Chem Mater 2015;27:3785–96.
[82] Corma A. From microporous to mesoporous molecular sieve materials and their use in catalysis. Chem Rev 1997;97:2373–419.
[83] Solís-Fernández P, Rozada R, Paredes JI, Villar-Rodil S, Fernández-Merino MJ, Guardia L, et al. Chemical and microscopic analysis of graphene prepared by different reduction degrees of graphene oxide. J Alloys Compd 2012;536:S532–7.
[84] Wang H, Maiyalagan T, Wang X. Review on recent progress in nitrogen-doped graphene: synthesis, characterization, and its potential applications. ACS Catal 2012;2:781–94.
[85] Zhao Q, Li Y, Liu R, Chen A, Zhang G, Zhang F, et al. Enhanced hydrogenation of olefins and ketones with a ruthenium complex covalently anchored on graphene oxide. J Mater Chem A 2013;1:15039–45.
[86] Zhu Y, Murali S, Cai W, Li X, Suk JW, Potts JR, et al. Graphene and graphene oxide: synthesis, properties, and applications. Adv Mater 2010;22:3906–24.
[87] Ferrari AC, Basko DM. Raman spectroscopy as a versatile tool for studying the properties of graphene. Nat Nanotechnol 2013;8:235–46.
[88] Casiraghi C, Hartschuh A, Qian H, Pliscanec S, Georgia C, Fasoli A, et al. Raman spectroscopy of graphene edges. Nano Lett 2009;9:1433–41.
[89] Gao W, Alemany LB, Ci L, Ajayan PM. New insights into the structure and reduction of graphite oxide. Nat Chem 2009;1:403–8.
[90] Brewer GJ. Alzheimer's disease causation by copper toxicity and treatment with zinc. Front Aging Neurosci 2014;6.
[91] Brown MJ, Margolis S. Lead in drinking water and human blood lead levels in the United States. Morb Mortal Wkly Rep Surveill Summ 2012;61(Suppl.):1–9 [Washington, D.C.: 2002].
[92] Del Toral MA, Porter A, Schock MR. Detection and evaluation of elevated lead release from service lines: a field study. Environ Sci Technol 2013;47:9300–7.
[93] Zhang Y, Zhang Q, Shi Q, Cai Z, Yang Z. Acid-treated g-C_3N_4 with improved photocatalytic performance in the reduction of aqueous Cr(VI) under visible-light. Sep Purif Technol 2015;142:251–7.
[94] Jung C, Heo J, Han J, Her N, Lee S, Oh J, et al. Hexavalent chromium removal by various adsorbents: powdered activated carbon, chitosan, and single/multi-walled carbon nanotubes. Sep Purif Technol 2013;106:63–71.
[95] Clancy TM, Hayes KF, Raskin L. Arsenic waste management: a critical review of testing and disposal of arsenic-bearing solid wastes generated during arsenic removal from drinking water. Environ Sci Technol 2013;47:10799–812.

[96] Sharma VK, Dutta PK, Ray AK. Review of kinetics of chemical and photocatalytical oxidation of Arsenic(III) as influenced by pH. J Environ Sci Health A Tox Hazard Subst Environ Eng 2007;42:997–1004.
[97] Jain A, Sharma VK, Mbuya OS. Removal of arsenite by Fe(VI), Fe(VI)/Fe(III), and Fe(VI)/Al(III) salts: effect of pH and anions. J Hazard Mater 2009;169:339–44.
[98] Sharma VK, Sohn M. Aquatic arsenic: toxicity, speciation, transformations, and remediation. Environ Int 2009;35:743–59.
[99] Frisbie SH, Mitchell EJ, Sarkar B. Urgent need to reevaluate the latest World Health Organization guidelines for toxic inorganic substances in drinking water. Environ Health Global Access Sci Sour 2015;14:63.
[100] Scheuhammer A, Braune B, Chan HM, Frouin H, Krey A, Letcher R, et al. Recent progress on our understanding of the biological effects of mercury in fish and wildlife in the Canadian Arctic. Sci Total Environ 2015;509–510:91–103.
[101] Chételat J, Amyot M, Arp P, Blais JM, Depew D, Emmerton CA, et al. Mercury in freshwater ecosystems of the Canadian Arctic: recent advances on its cycling and fate. Sci Total Environ 2015;509–510:41–66.
[102] Li P, Du B, Chan HM, Feng X. Human inorganic mercury exposure, renal effects and possible pathways in Wanshan mercury mining area, China. Environ Res 2015;140:198–204.
[103] Tang W, Zeng G, Gong J, Liang J, Xu P, Zhang C, et al. Impact of humic/fulvic acid on the removal of heavy metals from aqueous solutions using nanomaterials: a review. Sci Total Environ 2014;468-469:1014–27.
[104] Yan H, Li H, Tao X, Li K, Yang H, Li A, et al. Rapid removal and separation of iron(II) and manganese(II) from micropolluted water using magnetic graphene oxide. ACS Appl Mater Interfaces 2014;6:9871–80.
[105] Chen B, Ma Q, Tan C, Lim T, Huang L, Zhang H. Carbon-based sorbents with three-dimensional architectures for water remediation. Small 2015;11:3319–36.
[106] Kumar R, Chawla J, Kaur I. Removal of cadmium ion from wastewater by carbon-based nanosorbents: a review. J Water Health 2015;13:18–33.
[107] Cong H, Chen J, Yu S. Graphene-based macroscopic assemblies and architectures: an emerging material system. Chem Soc Rev 2014;43:7295–325.
[108] Cong H, Ren X, Wang P, Yu S. Macroscopic multifunctional graphene-based hydrogels and aerogels by a metal ion induced self-assembly process. ACS Nano 2012;6:2693–703.
[109] Huang Z, Zheng X, Lv W, Wang M, Yang Q, Kang F. Adsorption of lead(II) ions from aqueous solution on low-temperature exfoliated graphene nanosheets. Langmuir 2011;27:7558–62.
[110] Zhang M, Gao B, Cao X, Yang L. Synthesis of a multifunctional graphene–carbon nanotube aerogel and its strong adsorption of lead from aqueous solution. RSC Adv 2013;3:21099–105.
[111] Ren X, Li J, Tan X, Wang X. Comparative study of graphene oxide, activated carbon and carbon nanotubes as adsorbents for copper decontamination. Dalton Trans 2013;42:5266–74.
[112] Li J, Zhang S, Chen C, Zhao G, Yang X, Li J, et al. Removal of Cu(II) and fulvic acid by graphene oxide nanosheets decorated with Fe_3O_4 nanoparticles. ACS Appl Mater Interfaces 2012;4:4991–5000.
[113] Kumar S, Nair RR, Pillai PB, Gupta SN, Iyengar MAR, Sood AK. Graphene oxide–$MnFe_2O_4$ magnetic nanohybrids for efficient removal of lead and arsenic from water. ACS Appl Mater Interfaces 2014;6:17426–36.
[114] Li L, Zhou G, Weng Z, Shan X, Li F, Cheng H. Monolithic Fe_2O_3/graphene hybrid for highly efficient lithium storage and arsenic removal. Carbon 2014;67:500–7.
[115] Yang X, Shi Z, Liu L. Adsorption of Sb(III) from aqueous solution by QFGO particles in batch and fixed-bed systems. Chem Eng J 2015;260:444–53.
[116] Guo L, Ye P, Wang J, Fu F, Wu Z. Three-dimensional Fe_3O_4–graphene macroscopic composites for arsenic and arsenate removal. J Hazard Mater 2015;298:28–35.
[117] Cui L, Wang Y, Gao L, Hu L, Yan L, Wei Q, et al. EDTA functionalized magnetic graphene oxide for removal of Pb(II), Hg(II), and Cu(II) in water treatment: adsorption mechanism and sorption capacity. Chem Eng J 2015;281:1–10.
[118] Cui L, Wang Y, Gao L, Hu L, Wei Q, Du B. Removal of Hg(II) from aqueous solution by resin loaded magnetic beta-cyclodextrin bead and graphene oxide sheet: synthesis, adsorption mechanism and separation properties. J Colloid Interface Sci 2015;456:42–9.
[119] Cui L, Guo X, Wei Q, Wang Y, Gao L, Yan L, et al. Removal of mercury and methylene blue from aqueous solution by xanthate functionalized magnetic graphene oxide: sorption kinetic and uptake mechanism. J Colloid Interface Sci 2015;439:112–20.
[120] Lei Y, Chen F, Luo Y, Zhang L. Three-dimensional magnetic graphene oxide foam/Fe_3O_4 nanocomposite as an efficient absorbent for Cr(VI) removal. J Mater Sci 2014;49:4236–45.
[121] Sharma DC, Forster CF. A preliminary examination into the adsorption of hexavalent chromium using low-cost adsorbents. Bioresour Technol 1994;47:257–64.
[122] Lee S, Kim W, Laldawngliana C, Tiwari D. Removal behavior of surface modified sand for Cd(II) and Cr(VI) from aqueous solutions. J Chem Eng Data 2010;55:3089–94.
[123] Cao C, Cui Z, Chen C, Song W, Cai W. Ceria hollow nanospheres produced by a template-free microwave-assisted hydrothermal method for heavy metal ion removal and catalysis. J Phys Chem C 2010;114:9865–70.
[124] Cao C, Qu J, Yan W, Zhu J, Wu Z, Song W. Low-cost synthesis of flowerlike a-Fe_2O_3 nanostructures for heavy metal ion removal: adsorption property and mechanism. Langmuir 2012;28:4573–9.
[125] Li S, Lu X, Xue Y, Lei J, Zheng T, Wang C. Fabrication of polypyrrole/graphene oxide composite nanosheets and their applications for Cr(VI) removal in aqueous solution. PLoS ONE 2012;7.
[126] Ai Z, Cheng Y, Zhang L, Qiu J. Efficient removal of Cr(VI) from aqueous solution with Fe@Fe_2O_3 core–shell nanowires. Environ Sci Technol 2008;42:6955–60.
[127] Wang H, Yuan X, Wu Y, Zeng G, Chen X, Leng L, et al. Facile synthesis of amino-functionalized titanium metal-organic frameworks and their superior visible-light photocatalytic activity for Cr(VI) reduction. J Hazard Mater 2015;286:187–94.
[128] Liu Y, Luo C, Cui G, Yan S. Synthesis of manganese dioxide/iron oxide/graphene oxide magnetic nanocomposites for hexavalent chromium removal. RSC Adv 2015;5:54156–64.
[129] Vadahanambi S, Jung J, Oh I. Microwave syntheses of graphene and graphene decorated with metal nanoparticles. Carbon 2011;49:4449–57.
[130] Chen X, Chen B. Macroscopic and spectroscopic investigations of the adsorption of nitroaromatic compounds on graphene oxide, reduced graphene oxide, and graphene nanosheets. Environ Sci Technol 2015;49:6181–9.
[131] Yan H, Wu H, Li K, Wang Y, Tao X, Yang H, et al. Influence of the surface structure of graphene oxide on the adsorption of aromatic organic compounds from water. ACS Appl Mater Interfaces 2015;7:6690–7.
[132] Turco A, Malitesta C, Barillaro G, Greco A, Maffezzoli A, Mazzotta E. A magnetic and highly reusable macroporous superhydrophobic/superoleophilic PDMS/MWNT nanocomposite for oil sorption from water. J Mater Chem A 2015;3:17685–96.
[133] Shi P, Ye N. Investigation of the adsorption mechanism and preconcentration of sulfonamides using a porphyrin-functionalized Fe_3O_4–graphene oxide nanocomposite. Talanta 2015;143:219–25.
[134] Li Y, Wu X, Li Z, Zhong S, Wang W, Wang A, et al. Fabrication of $CoFe_2O_4$–graphene nanocomposite and its application in the magnetic solid phase extraction of sulfonamides from milk samples. Talanta 2015;144:1279–86.
[135] Chowdhury I, Duch MC, Mansukhani ND, Hersam MC, Bouchard D. Interactions of graphene oxide nanomaterials with natural organic matter and metal oxide surfaces. Environ Sci Technol 2014;48:9382–90.
[136] Fan W, Gao W, Zhang C, Tjiu WW, Pan J, Liu T. Hybridization of graphene sheets and carbon-coated Fe_3O_4 nanoparticles as a synergistic adsorbent of organic dyes. J Mater Chem 2012;22:25108–15.
[137] Wu Q, Feng C, Wang C, Wang Z. A facile one-pot solvothermal method to produce superparamagnetic graphene–Fe_3O_4 nanocomposite and its application in the removal of dye from aqueous solution. Colloids Surf B Biointerfaces 2013;101:210–4.
[138] Wang S, Wei J, Lv S, Guo Z, Jiang F. Removal of organic dyes in environmental water onto magnetic–sulfonic graphene nanocomposite. Clean Soil Air Water 2013;41:992–1001.
[139] Li J, Shao Z, Chen C, Wang X. Hierarchical GOs/Fe_3O_4/PANI magnetic composites as adsorbent for ionic dye pollution treatment. RSC Adv 2014;4:38192–8.
[140] Liu X, Yan L, Yin W, Zhou L, Tian G, Shi J, et al. A magnetic graphene hybrid functionalized with beta-cyclodextrins for fast and efficient removal of organic dyes. J Mater Chem A 2014;2:12296–303.
[141] Namvari M, Namazi H. Synthesis of magnetic citric-acid-functionalized graphene oxide and its application in the removal of methylene blue from contaminated water. Polym Int 2014;63:1881–8.
[142] Sun J, Liao Z, Si R, Kingori GP, Chang F, Gao L, et al. Adsorption and removal of triphenylmethane dyes from water by magnetic reduced graphene oxide. Water Sci Technol 2014;70:1663–9.
[143] Kyzas GZ, Deliyanni EA, Matis KA. Graphene oxide and its application as an adsorbent for wastewater treatment. J Chem Technol Biotechnol 2014;89:196–205.
[144] Zeng S, Gan N, Weideman-Mera R, Cao Y, Li T, Sang W. Enrichment of polychlorinated biphenyl 28 from aqueous solutions using Fe_3O_4 grafted graphene oxide. Chem Eng J 2013;218:108–15.
[145] Sinha A, Jana NR. Graphene-based composite with γ-Fe_2O_3 nanoparticle for the high-performance removal of endocrine-disrupting compounds from water. Chem Asian J 2013;8:786–91.
[146] Bai X, Feng R, Hua Z, Zhou L, Shi H. Adsorption of 17ß-Estradiol (E2) and Pb(II) on Fe_3O_4/graphene oxide (Fe_3O_4/GO) nanocomposites. Environ Eng Sci 2015;32:370–8.
[147] Sereshti H, Samadi S, Asgari S, Karimi M. Preparation and application of magnetic graphene oxide coated with a modified chitosan pH-sensitive hydrogel: an efficient biocompatible adsorbent for catechin. RSC Adv 2015;5:9396–404.
[148] Mehdinia A, Khodaee N, Jabbari A. Fabrication of graphene/Fe_3O_4@polythiophene nanocomposite and its application in the magnetic solid-phase extraction of polycyclic aromatic hydrocarbons from environmental water samples. Anal Chim Acta 2015;868:1–9.
[149] Yang X, Li J, Wen T, Ren X, Huang Y, Wang X. Adsorption of naphthalene and its derivatives on magnetic graphene composites and the mechanism investigation. Colloids Surf Physicochem Eng Asp 2013;422:118–25.
[150] Chen W, Li S, Chen C, Yan L. Self-assembly and embedding of nanoparticles by in situ reduced graphene for preparation of a 3D graphene/nanoparticle aerogel. Adv Mater 2011;23:5679–83.
[151] Wu Z, Yang S, Sun Y, Parvez K, Feng X, Müllen K. 3D nitrogen-doped graphene aerogel-supported Fe_3O_4 nanoparticles as efficient electrocatalysts for the oxygen reduction reaction. J Am Chem Soc 2012;134:9082–5.
[152] Roy E, Patra S, Kumar D, Madhuri R, Sharma PK. Multifunctional magnetic reduced graphene oxide dendrites: synthesis, characterization and their applications. Biosens Bioelectron 2015;68:726–35.
[153] Byun J. Emerging frontiers of graphene in biomedicine. J Microbiol Biotechnol 2015;25:145–51.
[154] Chella S, Kollu P, Komarala EVPR, Doshi S, Saranya M, Felix S, et al. Solvothermal synthesis of $MnFe_2O_4$–graphene composite—investigation of its adsorption and antimicrobial properties. Appl Surf Sci 2015;327:27–36.
[155] Deng C, Gong J, Zeng G, Niu C, Niu Q, Zhang W, et al. Inactivation performance and mechanism of *Escherichia coli* in aqueous system exposed to iron oxide loaded graphene nanocomposites. J Hazard Mater 2014;276:66–76.

[156] Tian T, Shi X, Cheng L, Luo Y, Dong Z, Gong H, et al. Graphene-based nanocomposite as an effective, multifunctional, and recyclable antibacterial agent. ACS Appl Mater Interfaces 2014;6:8542–8.
[157] Zhan S, Zhu D, Ma S, Yu W, Jia Y, Yu H, et al. Highly efficient removal of pathogenic bacteria with magnetic graphene composite. ACS Appl Mater Interfaces 2015;7:4290–8.
[158] Ye S, Shao K, Li Z, Guo N, Zuo Y, Li Q, et al. Antiviral activity of graphene oxide: how sharp edged structure and charge matter. ACS Appl Mater Interfaces 2015;7:21571–9.
[159] Ma S, Zhan S, Jia Y, Zhou Q. Highly efficient antibacterial and Pb(II) removal effects of Ag–$CoFe_2O_4$–GO nanocomposite. ACS Appl Mater Interfaces 2015;7:10576–86.
[160] Chen J, Peng H, Wang X, Shao F, Yuan Z, Han H. Graphene oxide exhibits broad-spectrum antimicrobial activity against bacterial phytopathogens and fungal conidia by intertwining and membrane perturbation. Nanoscale 2014;6:1879–89.
[161] He J, Zhu X, Qi Z, Wang C, Mao X, Zhu C, et al. Killing dental pathogens using antibacterial graphene oxide. ACS Appl Mater Interfaces 2015;7:5605–11.
[162] Dinh NX, Chi DT, Lan NT, Lan H, Van Tuan H, Van Quy N, et al. Water-dispersible silver nanoparticles-decorated carbon nanomaterials: synthesis and enhanced antibacterial activity. Appl Phys A Mater Sci Process 2015;119:85–95.
[163] Moosavi R, Ramanathan S, Lee YY, Siew Ling KC, Afkhami A, Archunan G, et al. Synthesis of antibacterial and magnetic nanocomposites by decorating graphene oxide surface with metal nanoparticles. RSC Adv 2015;5:76442–50.
[164] Soroush A, Ma W, Silvino Y, Rahaman MS. Surface modification of thin film composite forward osmosis membrane by silver-decorated graphene-oxide nanosheets. Environ Sci Nano 2015;2:395–405.
[165] Nine MJ, Cole MA, Tran DNH, Losic D. Graphene: a multipurpose material for protective coatings. J Mater Chem A 2015;3:12580–602.
[166] Sun X, Qin J, Xia P, Guo B, Yang C, Song C, et al. Graphene oxide-silver nanoparticle membrane for biofouling control and water purification. Chem Eng J 2015;281:53–9.
[167] Mahmoudi E, Ng LY, Ba-Abbad MM, Mohammad AW. Novel nanohybrid polysulfone membrane embedded with silver nanoparticles on graphene oxide nanoplates. Chem Eng J 2015;277:1–10.
[168] Krishnamoorthy K, Jeyasubramanian K, Premanathan M, Subbiah G, Shin HS, Kim SJ. Graphene oxide nanopaint. Carbon 2014;72:328–37.
[169] Yang S, Chen L, Mu L, Ma P. Magnetic graphene foam for efficient adsorption of oil and organic solvents. J Colloid Interface Sci 2014;430:337–44.
[170] Low J, Cao S, Yu J, Wageh S. Two-dimensional layered composite photocatalysts. Chem Commun 2014;50:10768–77.